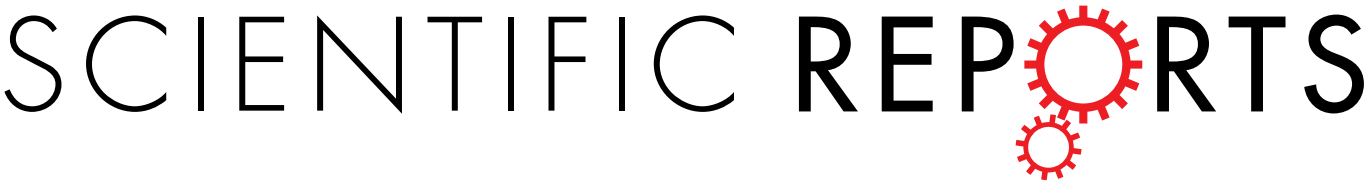

OPEN

β-adrenergic stimulation augments transmural dispersion of repolarization via modulation of delayed rectifier currents I_{Ks} and I_{Kr} in the human ventricle

Received: 12 July 2017
Accepted: 9 November 2017
Published online: 21 November 2017

C. Kang[1,2], A. Badiceanu[3], J. A. Brennan[1], C. Gloschat[1,2], Y. Qiao[1,2], N. A. Trayanova[3] & I. R. Efimov[1,2]

Long QT syndrome (LQTS) is an inherited or drug induced condition associated with delayed repolarization and sudden cardiac death. The cardiac potassium channel, I_{Kr}, and the adrenergic-sensitive cardiac potassium current, I_{Ks}, are two primary contributors to cardiac repolarization. This study aimed to elucidate the role of β-adrenergic (β-AR) stimulation in mediating the contributions of I_{Kr} and I_{Ks} to repolarizing the human left ventricle (n = 18). Optical mapping was used to measure action potential durations (APDs) in the presence of the I_{Ks} blocker JNJ-303 and the I_{Kr} blocker E-4031. We found that JNJ-303 alone did not increase APD. However, under isoprenaline (ISO), both the application of JNJ-303 and additional E-4031 significantly increased APD. With JNJ-303, ISO decreased APD significantly more in the epicardium as compared to the endocardium, with subsequent application E-4031 increasing mid- and endocardial APD80 more significantly than in the epicardium. We found that β-AR stimulation significantly augmented the effect of I_{Ks} blocker JNJ-303, in contrast to the reduced effect of I_{Kr} blocker E-4031. We also observed synergistic augmentation of transmural repolarization gradient by the combination of ISO and E-4031. Our results suggest β-AR-mediated increase of transmural dispersion of repolarization, which could pose arrhythmogenic risk in LQTS patients.

The QT interval is the time elapsed between ventricular depolarization and repolarization. A prolonged QT interval, caused by either drugs or genetic mutations, is termed Long QT syndrome (LQTS). It is well established that LQTS significantly increases the risk of sudden cardiac death from polymorphic ventricular tachycardia (VT), known as Torsade de Pointes (TdP)[1]. Over 50% of all LQTS patients face high risk of sudden cardiac death from VT. There are two distinct delayed rectifier potassium currents, rapid (I_{Kr}) and slow (I_{Ks}), which are primarily responsible for cardiac repolarization[2]. A majority of heritable LQTS cases, such as LQT1, LQT5, and LQT11, are associated with mutations in the KCNQ1 gene, which encodes I_{Ks}[3] or constituents of the I_{Ks} macromolecular complex[4,5]. However, in large mammals, it has been shown in certain studies that I_{Kr} is actually the dominant delayed rectifier potassium current where I_{Ks} only contributes relatively little to repolarization. Therefore, the generally accepted notion that I_{Ks} plays the biggest role in contributing to LQTS is puzzling[6,7]. Previous studies have demonstrated that I_{Ks} expression is highly variable in mammalian cells. For instance, guinea pig myocytes possess significant I_{Ks} current[2,8–10], but mouse, rat, canine, and rabbit myocytes have little to no I_{ks} current[11–13]. In human myocytes, though the I_{Ks} blockade does prolong the QT interval, the amplitude of I_{Ks} has been reportedly low in human ventricular myocytes[14–16]. To complicate the question of I_{Ks} contribution to repolarization in the human heart even further, researchers often face experimental difficulties in recording I_{Ks} due to the various methods of isolating myocytes from human tissue[17–19]. Overall, the apparent controversial evidence between many clinical and experimental studies raises concerns about our current understanding of the role of I_{Ks} in human repolarization.

[1]The George Washington University, Washington, DC, USA. [2]Washington University in St. Louis, St. Louis, MO, USA. [3]John Hopkins University, Baltimore, MD, USA. Correspondence and requests for materials should be addressed to I.R.E. (email: efimov@gwu.edu)

Organization	Age	Gender	BMI	Cause of Death	LVEF
MTS	38	M	18.2	Head Trauma	65%
MTS	63	F	22.51	CVA/Stroke	60%
MTS	19	M	30.42	Head Trauma	N/A
MTS	68	M	20.81	Head Trauma	N/A
MTS	68	M	18.13	CVA/Stroke	N/A
MTS	40	M	31.29	CVA/Stroke	N/A
MTS	59	F	19.92	CVA/Stroke	N/A
MTS	44	F	68.89	Anoxia	N/A
WRTC	76	M	45.6	CVA/ICH/Stroke	N/A
WRTC	57	M	28.4	CVA/ICH/Stroke	50–55%
WRTC	47	M	30.6	Anoxia	60%
WRTC	60	M	22.8	CVA/ICH/Stroke	N/A
WRTC	78	M	24.8	CVA/ICH/Stroke	N/A
WRTC	57	F	39.8	Anoxia	60–65%
WRTC	50	M	31.1	Anoxia	45%
WRTC	59	M	34.1	CVA/Stroke	N/A
WRTC	62	F	41	CVA/Stroke	65%

Table 1. Donor Heart Information. Hearts were acquired from Mid-America Transplant Services (MTS) and Washington Regional Transplant Community (WRTC). Age, gender, body mass index, and cause of death are listed for all hearts used in the study. Left ventricular ejection fraction (LVEF) was provided when echocardiography was performed and made available for transplant evaluation. Groups for separate protocols were not categorized with donor information provided. CVA: cerebrovascular accident; ICH: intracerebral hemorrhage. Anoxia refers to brain anoxia. No donor hearts from victims of sudden cardiac death were included.

In addition to our relatively limited understanding of the general contributions of I_{Kr} and I_{Ks} in human cardiac repolarization, the individual contributions of these two currents also still remains unclear. In guinea pig myocytes, these two cardiac potassium currents are dynamic and significantly depend on the type of adrenergic receptor stimulation[20]. Stimulation of $\beta_{1,2}$-adrenergic receptors is known to significantly augment I_{Ks}[9,21–23], whereas stimulation of β_3-AR actually decreases I_{Ks}[10]. Experimental evidence from guinea pig myocytes further suggests that the dominant repolarization current shifts from I_{Kr} to I_{Ks} during beta-adrenergic stimulation[20]. It remains unclear if this shift can be replicated in other mammalian models, such as humans, which have lower expression and thus a smaller contribution of I_{Ks}. Recently, we have shown that I_{Kr} is significantly reduced in humans with end stage heart failure (HF), thereby indicating the possible increased significance of I_{Ks}[24].

These numerous uncertainties and continued controversies pose a significant hurdle for computational models of mammalian, and especially human, action potentials. The three most frequently used models of human ventricular myocyte action potentials, ten Tusscher[25], Grandi[26], and O'Hara-Rudy[27], all behave differently under I_{Ks} or I_{Kr} blockade. Only the most recent O'Hara-Rudy model appears to most closely correlate with experimental data describing partial I_{Kr} block, yet early afterdepolarizations are present in the model and not observed in cardiac tissue experiments[28]. These discrepancies are detrimental to accurate predictions of arrhythmic risks. Following these lines of inquiry, we pursued a pharmacological investigation in the coronary perfused human left ventricular (LV) wedge preparation to examine the basal transmural contribution of I_{Ks} to repolarization, β-AR modulation of I_{Ks} and I_{Kr}, and changes in transmural dispersion of repolarization due to β-AR stimulation and potassium channel block. Finally, we adapted electrophysiological conditions into a computational human myocyte model to corroborate our experimental results with computational ones.

Methods

Donor heart procurement. Adult donor human hearts were procured from either Washington Regional Transplant Community (WRTC) in Washington, DC or from Mid-America Transplant Services (MTS) in St. Louis, MO. Experimental and tissue procurement protocols were approved by the Institutional Review Boards at The George Washington University in Washington, DC and Washington University in St. Louis, MO. Heart tissue was de-identified by the organ procurement organizations prior to being provided to the research team. Methods and protocols described in these studies were performed in accordance with federal human research guidelines. A complete list of hearts with body mass index (BMI), cause of death, and LV ejection fraction (LVEF, listed when available) used in study are presented in Table 1. In this study, we completely excluded any donor hearts from victims of sudden cardiac death. Anoxia refers to anoxia of the brain.

Prior to removal from the chest, explanted donor hearts procured by either WRTC or MTS were cardioplegically arrested after aortic cross-clamp through systematic perfusion. MTS hearts were transported (15–20 minutes) to the laboratory in ice cold high potassium solution (in mmol/L: NaCl 110, $CaCl_2$ 1.2, KCl 16, $MgCl_2$ 16, $NaHCO_3$ 10) to preserve the tissue. WRTC hearts were delivered approximately 2–3 hours post cross-clamp via courier in ice-cold commercial transplant preservation solution (Belzer UW) in the same manner as standard heart transplants. All hearts were categorized as non-failing donor hearts in line with all previously published data from our laboartory[29–31].

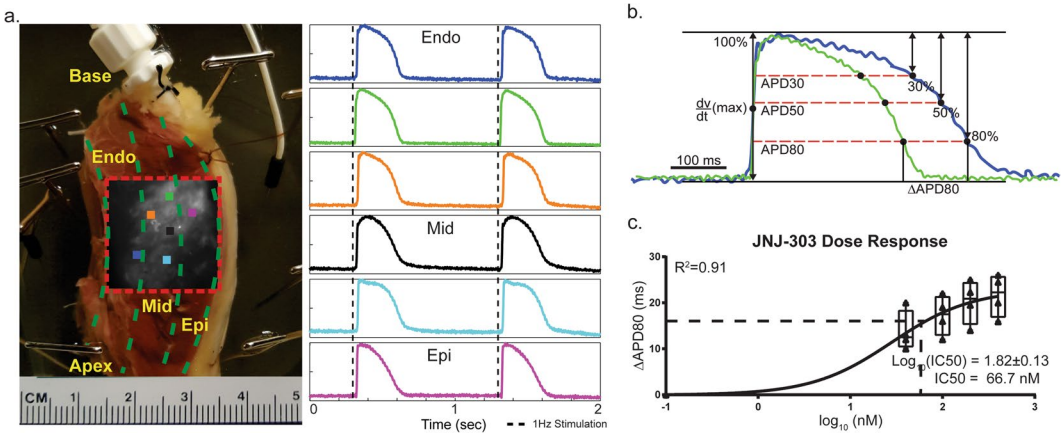

Figure 1. Experimental Preparations. Section of the left ventricular marginal area from a donor human hearts was dissected into a coronary perfused wedge preparation. (**a**) Orientation of the preparation was labeled accordingly. Color squares indicate recordings sites of the representative optical traces, illustrating that the tissue was fully perfused on the transmural surface. (**b**) Representative traces of how different repolarization % changes APD and ΔAPD between conditions were calculated. (**c**) A third order sigmoidal curve was fitted to ΔAPD80 vs Log (nM) for the dose response of JNJ-303. Log(IC50) was obtained as 1.82 ± 0.13 (±S.E.). 95% confidence interval for IC50 in nM was between 35.4 and 128.4 nM. Best fit value was determined to be 66.7 nM.

Experimental preparation. A coronary perfused section (wedge) from the marginal area of the LV (Fig. 1a) was dissected, cannulated, and electrically recovered as previously described[30]. The LV wedge was perfused with 37 °C oxygenated Tyrode's solution in a 3D printed tissue chamber during experimentation. Constant coronary flow pressure of ~60 mmHg was carefully maintained. The wedge preparation was washed with 2L of Tyrode's solution to remove any floating fat tissue or excess transplant solution, as well as to restore basal electrophysiology (EP)[31] conditions prior to beginning dye loading. Between 5–10 μM of the excitation-contraction uncoupler blebbistatin was loaded into the tissue and allowed to perfuse for 15 minutes to stop contractions. Then, 3–5 μM of a transmembrane potential sensitive dye, di-4-ANEPPS, was loaded into the tissue through an injection port. A thin slice of the transmural wall was removed following blebbistatin and dye loading to improve signal quality. Two sensing needle electrodes were placed on either side of the wedge preparation, and one grounding electrode was placed inside the perfusion chamber. A pseudo-ECG was recorded with Powerlab 26T (AD instruments) throughout the duration of the experiment (Supplemental Fig. 3). A platinum-iridium tipped bipolar pacing electrode was placed on the transmural surface within the field of view to accurately assess both longitudinal and transverse conduction. Optical action potentials were mapped from an approximately 1.5–2.0 cm × 1.5–2.0 cm field of view at the transmural surface of the wedge (Fig. 1a) using a MiCAM Ultima L CMOS camera with high spatial and temporal resolutions (100 × 100 pixels, 1,000 frames/sec; SciMedia, CA).

Electrophysiology experimental protocol. LV wedge preparations were studied under 3 different experimental protocols, labeled A, B, and C in Supplemental Fig. 1. Hearts procured from MTS were randomly selected for either a dose response protocol (n = 4, protocol A), or an I_{Ks} block protocol (n = 5, protocol B). Hearts procured from WRTC were used for a β-AR modulation of I_{Ks} and I_{Kr} block (n = 9, protocol C). In protocol C, the drugs were added at each step without washout, retaining the effect of previous agents. We applied a steady-state (S1-S1) restitution pacing protocol at twice the diastolic pacing threshold intensity to determine dependence of AP duration (APD) on pacing cycle length (PCL), which was progressively shortened from PCL = 2000 ms at 500, 200, and 100 ms intervals until the functional refractory period was reached. ISO (100 nM, Sigma Aldrich) was used for β-AR stimulation. JNJ-303 (200 nM, Sigma Aldrich) and E-4031 (1 μM, Sigma Aldrich) were used to selectively block I_{Ks} and I_{Kr}, respectively. In a study published previously, the tissue retains its EP properties for up to three hours while in an experimental bath[32].

Data processing. Rhythm, a custom-made MATLAB program designed for optical mapping data analysis, was used for calculating APD and plotting both activation and APD maps[33]. APs were filtered in space (3 × 3 pixel neighborhood) and time (low pass Butterworth filter at 100–150 Hz). Baseline fluorescent drift was removed with a first- or second-order fitted curve, as necessary. Activation times were determined by dV/dt_{max} and used to reconstruct activation maps and calculate conduction velocity (CV). APDs were calculated by measuring the elapsed time between activation and various repolarization percentages, as shown in Fig. 1b. For ease of comparison to previously published data from the human ventricular wedge[24,30,31], as well as drug effectiveness (Fig. 2), we used APD measured at 80% repolarization (APD80). Both APD80 and CV were collected and analyzed at the physiological stimulation frequency of 1 Hz. ORCA, a custom MATLAB analysis package[34], was modified and used for measurements of CV in the longitudinal and transverse directions (Fig. 3a). The directions were determined by the fastest and slowest CV from the pacing site (Supplemental Fig. 2).

Statistics analysis. Statistical analysis was performed using Prism 7 (GraphPad). Box-and-whisker plots with all data points presented were used for all quantitative comparisons. Significant differences were labeled

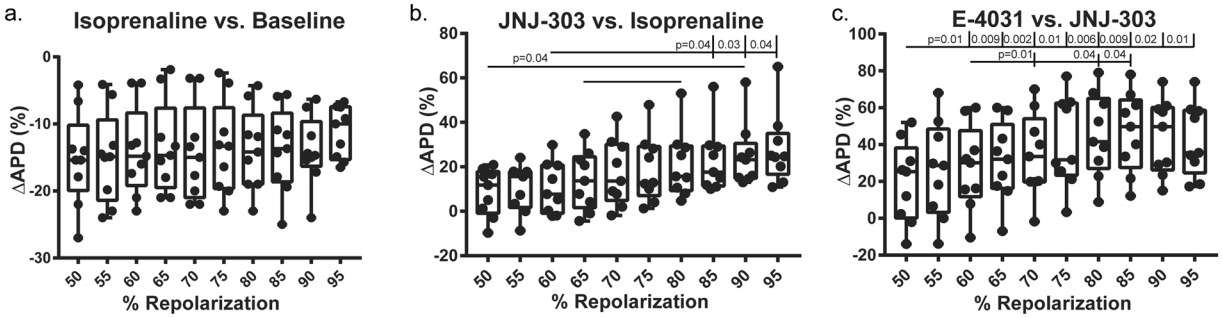

Figure 2. Percent Repolarization. Different pharmacologic interventions targeting specific ion channels led to changes in APD morphology. (**a**) Box-and-whisker (B&W) plots of % ΔAPD80 from baseline to isoprenaline indicate that APD did not alter among different % repolarization. (**b**) I_{Ks} blockade with JNJ-303 linearly increased % ΔAPD80 as % repolarization increased, indicating that I_{Ks} was more prominent at the latter phases of AP. (**c**) I_{Kr} block with E-4031 increased % ΔAPD80 as % repolarization was increased, peaking at approximately 80–85% to indicate that I_{Kr} contributes the most at 80–85% repolarization.

with individual p-values. Three different statistical tests were used in this study: Welch's t-test, repeated measures of one-way ANOVA with post hoc Tukey's honest significant difference for multiple comparisons (*RM 1way ANOVA THSD*), and two-way ANOVA with post hoc Tukey's honest significant difference for multiple comparisons (*2way ANOVA THSD*). Different tests were used as necessary and as indicated in the results section.

Computational simulations. The O'Hara-Rudy model of the human ventricular AP was used to perform computer simulations illustrating the EP behavior of a single cardiomyocyte under a protocol similar to the experimental one described above[27]. Similar to the model presented in Heijman *et al*., the model used in this study was adjusted to account for the protein kinase A (PKA) phosphorylation of eight different targets: ryanodine receptor, L-type calcium channel, phospholamban, I_{Ks}, I_{Na}, I_{NaK}, I_{Kur}, and troponin I, under both basal and β-stimulation conditions[35]. PKA phosphorylation was modeled as a binary process, where the given substrate was either considered phosphorylated or not phosphorylated. Therefore, the eight targets were divided into two subpopulations. At each time step, the current for a given substrate was computed by adding the currents passing through both phosphorylated and non-phosphorylated populations. The fraction of molecules allocated to each population was chosen so that the APs obtained from the simulations matched the ones recorded experimentally for both basal and β-AR stimulation conditions. The effects of JNJ-303 and E-4031 were modeled by setting the current through 80% of I_{Ks} channels and 20% of I_{Kr} channels equal to zero. The myocyte model was first paced at the physiological rate used in experimental tests (1 Hz) until steady state was reached, and the following 10 beats were recorded. APDs were computed for conditions like the experimental ones.

Results

Changes in APD at different degrees of repolarization. There are several definitions of APD used by experimentalists, with APD80 (APD at 80% of repolarization) being the most popular. In this study, we assessed how different pharmacologic interventions affected APD defined at different percentages of repolarization. Figure 2 shows changes in various APD percentages (from APD50 to APD95), caused by different pharmacologic interventions. β-AR stimulation shortened APD evenly across all APD percentages: from APD50 to APD95. ΔAPD during β-AR stimulation was fitted by a linear curve with an R^2 value of 0.62, and no significant difference in ΔAPD was observed among any repolarization percentages. JNJ-303 caused linearly increasing ΔAPD ($R^2 = 0.97$) as repolarization percentage increased. There were significant differences between lower and higher percentages of repolarization (50% vs. 90%, $p = 0.04$; 60% vs. 85%/90%/95% $p = 0.04$, $p = 0.03$, $p = 0.04$, respectively; *RM 1way ANOVA THSD*). Finally, ΔAPD vs. APD% caused by E4301 had a bell curve shape with a maximum value at ~APD80 to APD85. An exponential curve was used to fit this change ($R^2 = 0.15$). Significant differences were observed between 50% and 60 to 95% repolarization ($p = 0.01$, $p = 0.009$, $p = 0.002$, $p = 0.01$, $p = 0.006$, $p = 0.009$, $p = 0.02$, $p = 0.01$; *RM 1way ANOVA THSD*), as well as between 60 and 70/80/85% ($p = 0.01$, $p = 0.04$, $p = 0.04$, respectively; *RM 1way ANOVA THSD*).

β-AR stimulation significantly alters conduction properties. CV was calculated from protocols B and C with three pharmacological agents. The LV transmural surface exhibited a baseline longitudinal conduction velocity (CV_L) of 44.4 ± 2.1 cm/sec and 41.6 ± 1.1 cm/sec and a transverse conduction velocity (CV_T) of 24.6 ± 0.6 cm/sec and 23.5 ± 0.5 cm/sec, in protocols B and C, respectively. Conduction anisotropy (CV_L/CV_T) was 1.8 ± 0.1 and 1.7 ± 0.1, respectively. No difference in CV was observed in hearts acquired from different donor organizations. CV_L of 44.5 ± 2.4 cm/sec and CV_T of 25.8 ± 0.7 cm/sec were observed after acute application of JNJ-303, which produced an anisotropy ratio of 1.7 ± 0.1. No significant differences were observed in either CV ($p = 0.56$, $p = 0.99$; *2way ANOVA THSD*) or anisotropy ratios ($p = 0.64$; *Welch's t-test*) (Fig. 3d,e).

In protocol C, ISO significantly increased both CV_L and CV_T to 56.8 ± 1.8 cm/sec and 27.5 ± 0.7 cm/sec ($p < 0.0001$, $p = 0.0012$; *RM 1way ANOVA THSD*), respectively. This bidirectional increase of CV from baseline was mostly maintained through subsequent administration of JNJ-303 and E4031. CV_L and CV_T values after application of JNJ-303 were 54.1 ± 2.35 cm/sec and 28.2 ± 0.9 cm/sec, respectively. Both CV_L and CV_T remained

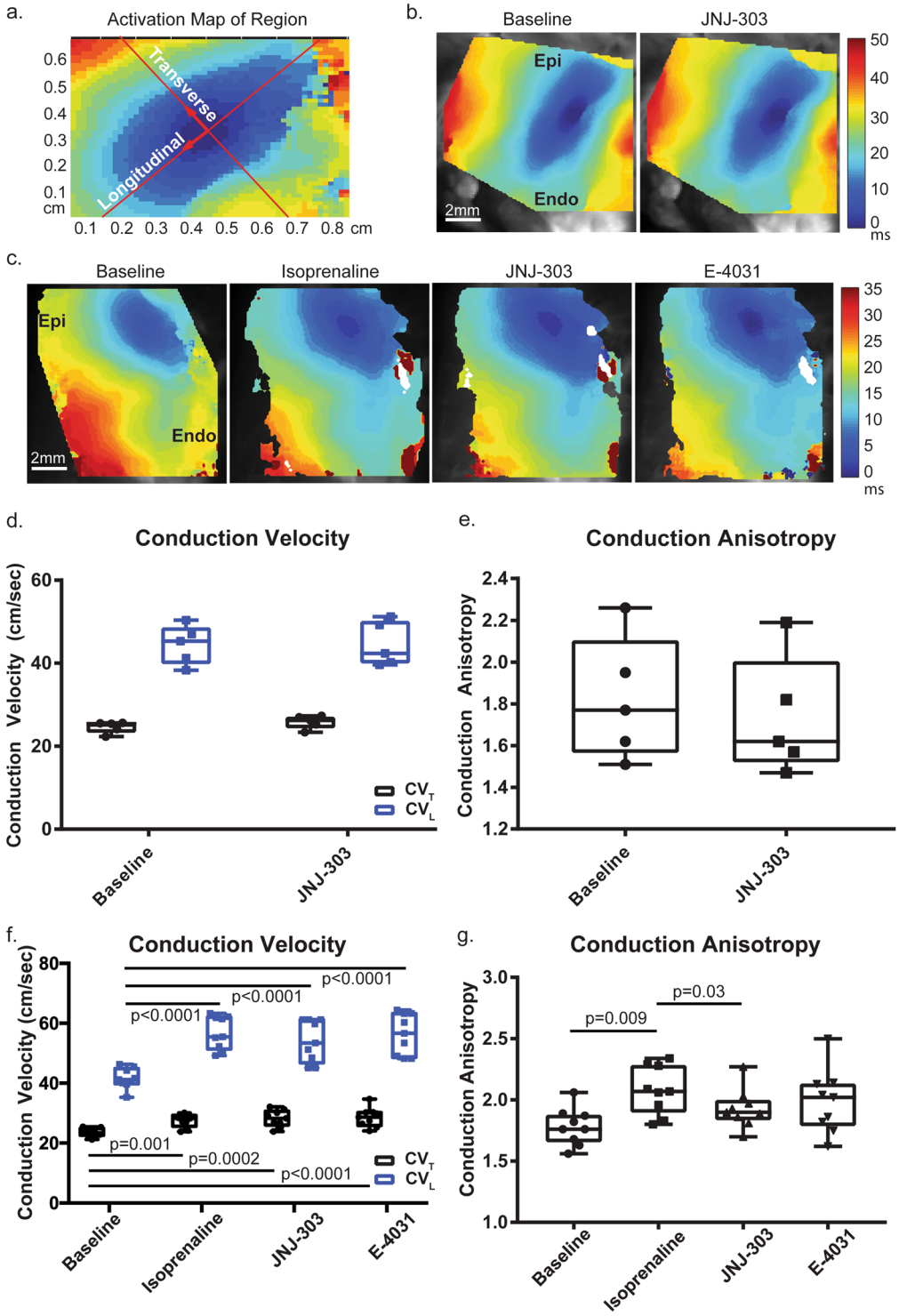

Figure 3. Conduction Properties. Conduction velocity (CV) was calculated from the transmural surface of the preparation. (**a**) A typical elliptical activation pattern was observed. Directions of activation (longitudinal, transverse) indicate the fastest and slowest conduction, respectively. (**b**) A representative activation map from protocol B shows that the activation pattern was the same both before and after application of JNJ-303. (**c**) Representative activation maps from protocol C indicate that conduction was increased with the application of isoprenaline. This change in activation was maintained with the addition of JNJ-303 and E-4031. (**d**) No significant difference was observed between transverse and longitudinal conduction velocities (CV_T, CV_L) in protocol B, and the anisotropy ratio was not altered (**d**). (**f**) Both CV_T and CV_L increased significantly with isoprenaline, but no other significant changes from previous conditions were observed. However, significant differences to the baseline were apparent. (**g**) Conduction anisotropy increased with isoprenaline, slightly decreased with JNJ-303, and remained unchanged with E-4031.

unchanged after final application of E4031(56.3 ± 2.3 cm/sec and 28.6 ± 1.0 cm/sec, respectively). The ratio of anisotropy was increased to 2.1 ± 0.2 after ISO, indicating that the increase of CV_L exceeded that of CV_T. This ratio was, however, significantly decreased to 1.9 ± 0.05 after JNJ-303 (p = 0.03, *RM 1way ANOVA THSD*). This decrease, though also observed in protocol B, did not reach statistical significance. Furthermore, additional application of E4031 did not significantly alter anisotropy (2.0 ± 0.08) (Fig. 3f,g).

β-AR stimulation modulates I_{Ks} and I_{Kr}. Subsequent APD analyses were based on results from previous sections. Our data showed that APD80 was indeed the optimal definition due to the effectiveness of measuring ΔAPD80 for both I_{Ks} and I_{Kr}. Furthermore, from protocol A, we determined that the log of IC50 for JNJ-303 in human ventricular tissue was 1.82 ± 0.13 (±S.E.) with 95% confidence interval for IC50 in nM between 35.4 and 128.4 nM (Fig. 1c). The best fit IC50 was 67 nM, which determined the saturation concentration of 200 nM which we used in protocols B and C.

Baseline APD80 for protocols A and B were 372 ± 16 ms and 342 ± 11 ms, respectively (averaged 354 ± 13), and 288 ± 13 ms (p = 0.0021; *Welch's t-test*) for protocol C (Supplemental Fig. 7), indicating basal differences in donor hearts from the two different geographical regions in the United States. Previous reports from isolated rat myocytes showed that β-AR stimulation significantly increased I_{Ks} and its relative contribution to the repolarization process[20,21,36]. Our study indicated a similar trend (Fig. 4). Isolated JNJ-303 slightly increased the APD80 to 363 ± 19 ms ms, a 21.4 ± 5.7 ms ms (or 6.5 ± 1.8%) prolongation (p = 0.47, *Welch's t-test*). One the other hand, in protocol C, ISO significantly reduced the APD80 to 249 ± 12 ms first (p = 0.004, *2way ANOVA THSD*). Subsequent addition of JNJ-303 dramatically increased the APD80 to 306 ± 17 ms (p = 0.002, *2way ANOVA THSD*), a 57.1 ± 9.6 ms (or 24.7 ± 4.3%) prolongation (p = 0.008 and p = 0.003; *Welch's t-test*). The final application of E-4031 further increased the APD80 to 463 ± 35 ms, a 157 ± 24 ms (or 51.3 ± 6.6%) prolongation. This change by E-4031 was most statistically significant compared to all previous conditions (p = 0.0009, p = 0.0003, p = 0.0009, *2way ANOVA THSD*). Previously published data from our laboratory using the same preparation documented an increase of approximately 65% when E-4031 was applied without any β-AR stimulation[24].

Shifts in restitution properties. APD restitution curves for each condition were fitted with a two-phase exponential curve starting from an S1–S1 of 300 ms to 2000 ms. In protocol B, the APD restitution curve was shifted slightly upward with the addition of JNJ-303. This upward shift brought the restitution curve above the baseline. In protocol C, the APD restitution curve was also shifted upward with the addition of JNJ-303, but it shifted downward with application of ISO. Addition of E-4031 dramatically shifted the curve upward. These same trends were observed when examining each transmural section separately (Fig. 5). The functional refractory period also changed in accordance with pharmacologic intervention (in ms): baseline 244 ± 13, ISO 203 ± 14, JNJ-303 309 ± 14, E-4031 385 ± 18. Significant differences were observed amongst all treatments (Fig. 5c).

Transmural dispersion of repolarization was altered by pharmacologic interrogation. Dispersion of repolarization across the transmural surface of the human LV was also characterized. APD80 maps and histograms (Fig. 4a–d) indicate that the APD increased from the epicardium to the endocardium. This gradient correlate to results already reported in both animal and human models. To quantitatively analyze the effects of pharmacologic intervention, the transmural surface was subdivided into three parts: endocardium, midmyocardium, and epicardium (Fig. 1a), similar to previous studies. Figure 6 shows ΔAPD80 in ms (% values shown in S\Supplemental Fig. 5). The percentage change of APD80 was calculated by $[(APD80_{Cond2} - APD80_{Cond1})/APD80_{Cond1}] * 100$. In protocol B, ΔAPD80 increased from epi to endo both in ms and % (epi: 16.2 ± 9.2 ms/5.2 ± 2.9%; mid: 21.4 ± 6.2 ms/6.5 ± 1.9%; endo: 25 ± 3.0 ms/7.4 ± 0.9%). However, this trend was not significant. Notably though, drug effects on the epicardium had the greatest variance, and this variance decreased toward the endocardium.

Transmural ΔAPD80 was shown first in protocol C (Fig. 6b). Here, ISO decreased APD more significantly in the epicardium as compared to the endocardium (epi: −52.3 ± 8.9 ms/−18.6 ± 2.9%; endo: −34.1 ± 8.1 ms/−11.1 ± 2.4%; P = 0.006, P = 0.008, respectively; *2way ANOVA THSD*). Midmyocardial ΔAPD80 fell in between these two values but was not significantly different from either (−43.8 ± 8.2 ms/−14.9 ± 2.6%). After administration of JNJ-303, this difference was abolished (epi: 61.6 ± 10 ms/27.6 ± 5.3%; mid: 59.3 ± 9.5 ms/24.3 ± 4.3%; endo: 57.8 ± 9.4 ms/22.1 ± 3.6%). However, the administration of E-4031 produced a significant transmural gradient in ΔAPD80. Both the midmyocardium and endocardium were significantly more affected as compared to the epicardium (epi: 139 ± 24 ms/46.5 ± 6.3%; mid: 161 ± 24 ms/53 ± 6.8%; endo: 172 ± 25 ms/53.3 ± 6.2%; p = 0.001, p < 0.0001; *2way ANOVA THSD*).

The transmural ΔAPD80 was also evident after normalization to the baseline APD (Fig. 6c). Similar significant differences were maintained. As ISO was the first drug administered to baseline, the comparison remains the same. JNJ-303 again abolished transmural ΔAPD80 gradient (epi, 15.8 ± 8 ms/6 ± 4.2%; mid, 16.7 ± 13 ms/6.5 ± 5.1%; endo 23.7 ± 10 ms/8.3 ± 3.9%). Finally, the application of E-4031 affected the midmyocardium and endocardium more than the epicardium (epi, 146 ± 21 ms/54.8 ± 8%; mid, 176 ± 27 ms/62.1 ± 8.9%; endo 195 ± 29 ms/66.1 ± 8.8%; p < 0.0001, p < 0.0001; *2way ANOVA THSD*). Interestingly, the endocardium also presented significantly increased % ΔAPD80 when compared to the midmyocardium (p = 0.01; *2way ANOVA THSD*).

Computational stimulation reflects experimental β-AR stimulation and I_{Ks} blockade. The computer model was calibrated to reproduce experimental APDs observed at the baseline and during β-AR stimulation (Fig. 7). The fractions of I_{Ks} and I_{Kr} channels phosphorylated by PKA during baseline conditions were set to 15%, while none of the other substrates were considered phosphorylated. During β-AR stimulation, all I_{Ks} and I_{Kr} channels and 25% of the other substrates were phosphorylated. The only exception was the L-type calcium

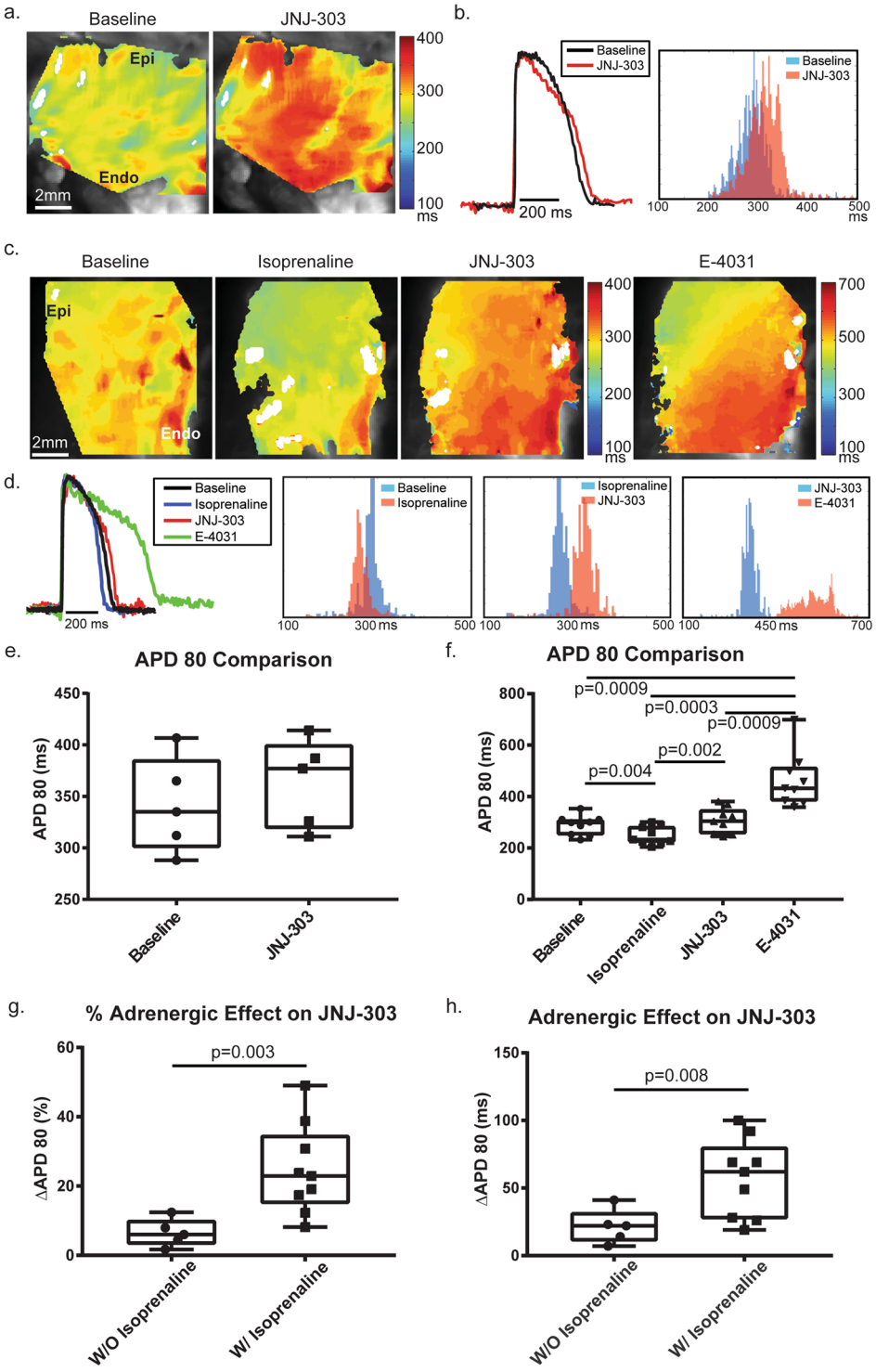

Figure 4. APD80 Comparisons. APD was measured at 80% of repolarization. (**a**) APD80 maps for both conditions in protocol B show that JNJ-303 increased APD80 slightly (but not significantly), as indicated by the red color. (**b**) Representative traces show changes in APD80 distribution after application of JNJ-303. Blue indicates baseline and red indicates the pharmacologic intervention. (**c**) APD80 maps for all conditions in protocol C highlight that isoprenaline decreased APD80, JNJ-303 increased APD80 above baseline, and E-4031 dramatically increased APD80. (**d**) Representative traces for each condition in protocol C show distribution histograms for three pairs of comparisons: baseline vs. isoprenaline, isoprenaline vs. JNJ-303, and JNJ-303 vs. E-4031. Bars in blue are representative of previous treatment, while bars in red are representative of post treatment. (**e**) B&W plots indicate a slight but not significant increase in APD80 with I_{Ks} block. (**f**) Significant reduction of APD80 was observed with application of isoprenaline, and an increase of APD80 was observed with both I_{Ks} and I_{Kr} block. (**g**,**h**) ΔAPD80 in both ms and % of pre and post JNJ-303 with or without isoprenaline stimulated β-ARs. ΔAPD80 drastically increased in both cases. See text for details.

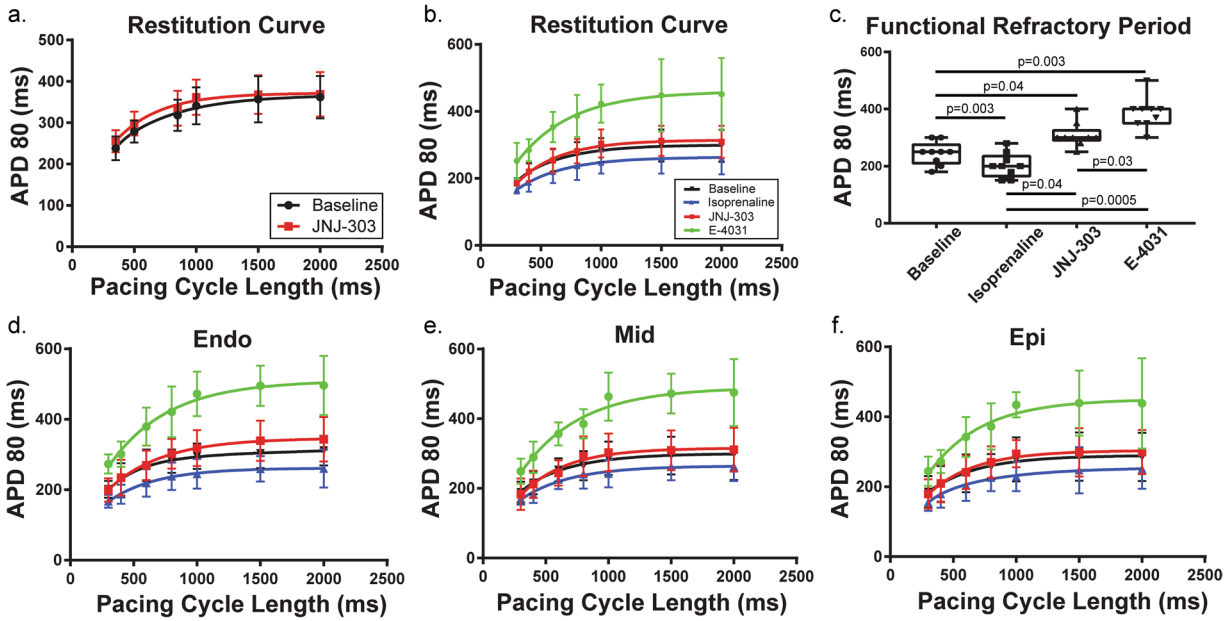

Figure 5. Restitution Properties. Using an S1S1 pacing protocol, restitution curves show that APD80 decreased as pacing cycle length decreased. This relationship was fitted using a two phase exponential curve. (**a**) The restitution curve shifted minimally with the addition of JNJ-303 in isolation. (**b**) Restitution downshifted with isoprenaline, upshifted with I_{Ks} block, and further upshifted with I_{Kr} block. (**c**) Functional refractory period was reached when S1S1 pacing lost capture. The refractory period significantly decreased with isoprenaline, and increased with both I_{Ks} and I_{Kr} blockers. (**d**–**f**) Restitution curves were plotted for endo, mid, and epi areas of the transmural surface indicating similar changes across all three areas.

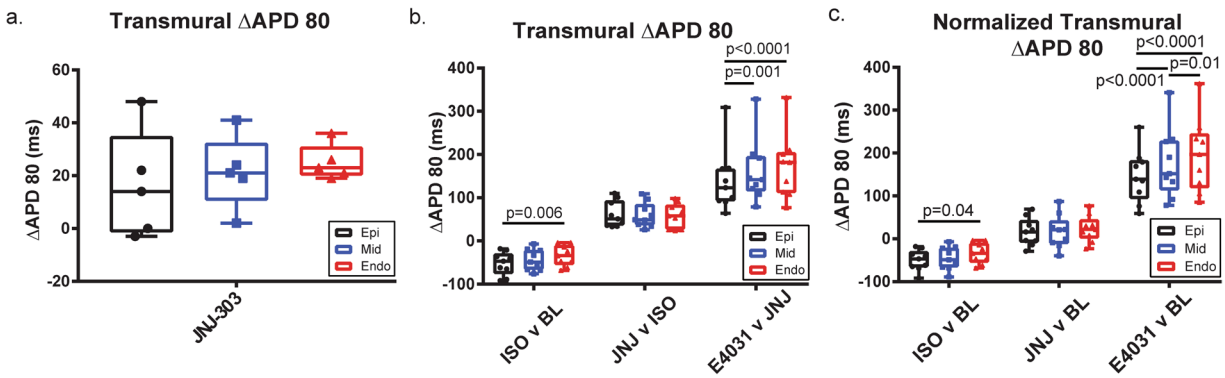

Figure 6. Transmural Dispersion. Absolute ΔAPD80 was calculated in milliseconds from epi, mid, and endo areas of the transmural surface. (**a**) No significant difference was observed from ΔAPD80 across the transmural surface post I_{Ks} blockade in protocol B. (**b**) ΔAPD80 was calculated as the difference between post and pre-treatment. APD80 reduction from isoprenaline was significantly greater in the epicardium as compared to the endocardium. On the other hand, APD80 under I_{Kr} blockade increased more significantly in the midmyocardium and endocardium as compared to the epicardium. (**c**) Normalized ΔAPD80 was calculated as the difference between post treatment and baseline. The transmural gradient was increased by both isoprenaline and E-4031, a trend which was also observed in comparing pre- and post-treatments.

channels, for which only 10% of the molecules were phosphorylated. This caused stimulated APD80 to shorten by 8.5%. After fixing these conditions, an 80% I_{Ks} block was applied to replicate an APD prolongation similar to that seen in experimental data, which is equivalent to a 14.6% increase in APD80. Experimental data for I_{Kr} could not be replicated due to occurrence of EADs following 20% or higher block (13.8% increase in APD80 from previous conditions).

Discussion

Summary of findings. For the first time, this study examined the role of β-AR stimulation in human LV repolarization, including modulation of its transmural dispersion. Our data indicates that the delayed rectifier repolarization potassium currents, $I_{K,}$ may be strongly modulated by β-AR in humans. Under baseline conditions

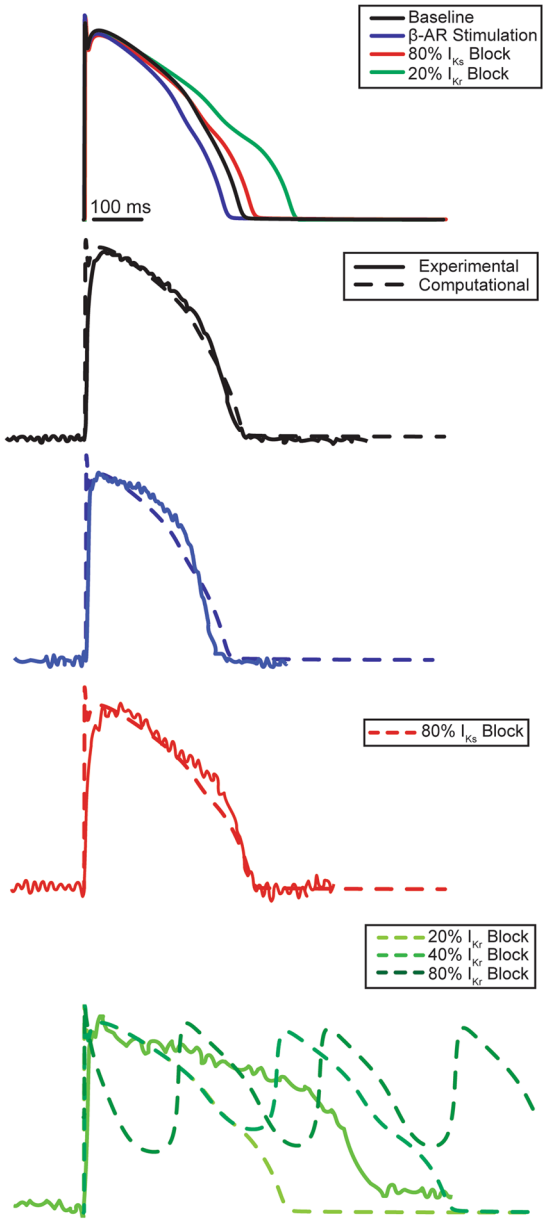

Figure 7. Computational Modeling of I_{Ks} and I_{Kr} Block with β-AR Stimulation. Protocol C was repeated in a computational model. The top panel displays AP traces obtained by sequential application of various pharmacologic interventions in the model. Baseline experimental AP traces were accurately reproduced by the model. β-AR stimulation was produced by an increased phosphorylation of all ion channels. The Model was also able to reproduce experimental data for I_{Ks} block at 80% current blockade. However, I_{Kr} blockade could not be reproduced using the modified O'Hara-Rudy model. When I_{Kr} block exceeded 20% early afterdepolarizations (EAD) were observed. EADs were not observed in any preparation even after saturated I_{Kr} block.

(in absence of β-AR stimulation), I_{Kr} is the predominant component of human LV repolarization. I_{Ks} is still present in the human LV, but it is relatively small. In this study, we observed that β-AR stimulation significantly increased the contribution of I_{Ks} to human LV repolarization. Moreover, combined β-AR stimulation and block of potassium channels resulted in significant transmural dispersion of repolarization, which is a known substrate for arrhythmias. Specifically, this study determined the acute effects of a specific I_{Ks} blocker, JNJ-303, on human LV repolarization, both with and without β-AR stimulation. At baseline conditions, JNJ-303 had no effect on CV (as expected), but it slightly increased APD80. β-AR stimulation significantly increased the activation of I_{Ks}, which was evident from a far more dramatic prolongation of APD80 produced by the application of JNJ-303 while under the effects of ISO. However, I_{Kr} block by application of E-4031 had a lesser effect on APD80 as compared to our previously reported data without β-AR stimulation[24], suggesting a reduction of I_{Kr} contribution to human LV repolarization during β-AR stimulation. Furthermore, we identified regional EP differences among donor hearts; hearts acquired in St. Louis exhibited significantly longer APD values as compared to hearts acquired in

Washington DC, while no difference in CV was observed. This difference in the APD can be attributed to different institution's surgical procedure and supplies, namely cardioplegia, as well as differences in transportation time from the operating room to the laboratory.

β-AR stimulation increased tissue anisotropy. In healthy human hearts, β-AR receptors primarily activate G_s protein, which in turn, activates adenylyl cyclase pathway converting adenosine triphosphate (ATP) to cyclic adenosine monophosphate (cAMP). Increased cAMP concentrations lead to an increased activation of PKA. Through PKA phosphorylation of the principal gap junction protein connexin 43 (Cx43) and inward sodium channels (I_{Na}), CV is increased. ISO, a non-selective β-AR agonist, effectively increased both CV_T and CV_L, as well as the anisotropy ratio. In healthy tissues, Cx43 is localized at the ends of the myocytes, and lateralization of Cx43 is minimal[37]. I_{Na} also tends to localize to the cell ends[38]. The greater increase in longitudinal CV_L by β-AR stimulation can be explained by this localization.

Choice of pharmacologic agents and concentration. The concentrations of drugs used in this study were comparable to those published previously. 1 μM E-4031 has shown to completely block I_{Kr} channels, and this amount was used in previous studies published by our laboratory[12,24]. Many I_{Ks} blockers have also been used in past studies; for example, benzopyran chromanol 293B and its more potent analogues (HMR-1556, L-768,673, and BMS-208,782) are frequently used in animal models[14,39]. Studies have concluded that these I_{Ks} blockers do not directly induce arrhythmias in the respective models[40]. However, in some models, the addition of I_{Ks} blockers in concentrations that usually do not affect hERG can still prolong the QT interval and reproducibly cause LQT1-type TdP with ISO[41]. JNJ-303, a more recently developed specific I_{Ks} blocker, has a significantly reduced effect on I_{Kr} as compared to other previously used agents. JNJ-303 has been reported to not markedly affect I_{Kr}, prolong APD, nor induce EADs below a concentration of 10 μM[14]. The best fit IC_{50} from our human sample was approximately 67 nM, which is close to the previously reported 64 nM[14]. We selected 200 nM for comparison studies because it saturates the I_{Ks} blockade but is safe from triggering much more significant QT prolongation via binding to hERG.

Percent repolarization reflects alteration of APD morphology. In accordance with their names, the rapid and slow rectifier potassium currents contribute to AP repolarization in a consecutive fashion. ISO activates PKA through the signaling cascade described above, which then phosphorylates several different ionic channels and pumps as evident from both an observed increase in CV and shortening of APD. Since PKA phosphorylation is not selective, % ΔAPD does not vary with the definition of % repolarization at which the APD was measured. Being the slower component of the rectifying current, I_{Ks} predominately affects the latter portion of repolarization. The observed linear increase of % ΔAPD across different % repolarizations corroborated this idea. Conversely, the rapid component, I_{Kr}, most prominently affected % ΔAPD at 80 to 85% repolarization before its effect dropped off at higher percentages of repolarization. These results are evident from the I_{Kr} blocker having the largest impact on APD80 to APD85, while the I_{Ks} blocker most affected APD95. With most recording methods, APD95 to APD100 are typically not reliable due to noise, thus APD80 to APD85 were determined to be the best definitions of APD for studies of human I_{Ks} and I_{Kr}.

Impact of increased I_{Ks} in the human left ventricle. It is well established that I_{Kr} and I_{Ks} both play major roles in cardiac repolarization of large mammals. However, expression and relative contribution of I_{Ks} varies from study to study and from animal model to model[28,39,42]. Similar to the results observed in canine and rabbit myocytes studies, the specific I_{Ks} blocker at a saturated specific binding concentration of 200 nM did not significantly increase AP duration. The increase of APD, while detectable, was relatively minor.

An increased response to I_{Ks} block or increased I_{Ks} after β-AR stimulation has been widely reported in canine and guinea pig myocytes[20–23]. Response in humans, however, has not been well documented, especially in intact tissue. Rate dependency of I_{Ks} and I_{Kr} deactivation has also been previously reported, yet this continues to be debated. Using restitution pacing, we found that APD prolongation in the human left ventricle was not dramatically altered in relation to the pacing rate throughout the transmural surface. This finding is similar to what has been found in canine tissue. Canine studies have shown that specific $\beta_{1,2}$-AR stimulation increases I_{Ks}, an observation of which has been further corroborated in guinea pig studies[36]. β_1- and β_2-AR are two G protein-coupled receptors in the heart which allow for the activation of various signaling pathways for diverse cellular responses. β_1-AR primarily binds to G_s, whereas β_2-AR can bind to either G_i or G_s in healthy tissue, depending on the PKA-dependent phosphorylation. Therefore, the effect of β_2-stimulation on I_{Ks} is dependent on PKA activity β_3-AR is a third beta isoform which acutely activates a separate signaling pathway through the G_q-protein and decreases I_{Ks}[10]. Since there is a relatively low abundance β_3-AR in the healthy human heart though, the non-specific β-AR agonist primarily activates the dominant isoform (β_1-AR) which is coupled to the G_s protein. Still, the effect of isolated β_2-stimulation of human I_{Ks} has yet to be elucidated. For this reason, it would be worthwhile to examine the effects of isolated β_1- and β_2-AR stimulation on I_{Ks}, especially in considering the reversal of β_1- versus β_2-AR signaling during heart failure and concomitant slowing of repolarization[31,43].

β-AR stimulation alters contribution of delay rectifier potassium currents. The relative contribution of the two rectifier currents to repolarization has been debated. I_{Kr} is generally considered the dominant repolarizing current, yet mutations in I_{Ks}-related genes are responsible for three of the most common LQTS cases: LQT1, LQT5, and LQT11[3,4,44]. Unfortunately, most published studies have only examined a single current at a time in isolated myocytes. Recently developed individual cell techniques, such as "onion-peeling" or "dynamic clamping", can record multiple currents in the same cell[20,45–47]. Results of these new techniques are quite exciting. Studies of guinea pig repolarizing currents using the onion-peeling technique have suggested that different

catecholamine levels alter the contribution of the two potassium currents. Under 30 nM of ISO, it was shown that I_{Kr} remains unchanged and I_{Ks} increases dramatically, far surpassing I_{Kr} in its relative contribution to repolarization[20]. As discussed in the previous section, our data shows that ISO increased the impact of the I_{Ks} blockade, indicating a greater contribution from I_{Ks}. Our study also showed that the I_{Kr} blocker E-4031 had less of an effect after β-AR stimulation than what was observed in previously published data without such stimulation at the same drug concentration[24]. Thus, we report novel findings of a shift in balance of delayed rectifier potassium channels in human, results of which are critical to understanding causes of sudden cardiac death in LQT1 patients during beta-adrenergic stimulation.

Enhanced transmural dispersion via β-stimulation and I_{Kr} blockade. Transmural dispersion of repolarization has been shown to be a powerful functional substrate for arrhythmogenesis. It has widely been reported in coronary perfused wedge studies of different animal and human models that APD increases from epi- to endocardium[30,31,42]. Under normal conditions, this dispersion of APD is small and benign. Our study examined how pharmacologic interrogation increases this dispersion and potentially contributes to a functional block. β-AR stimulation decreased APD more dramatically in the epicardial region as compared to the midmyocardium and endocardium. While the β_1 receptor density is reportedly even across the transmural surface of normal hearts, it is known to decrease drastically in the endocardium during HF[48]. On the other hand, we observed that I_{Kr} block had a significantly stronger effect on APD in the endocardium as compared to the midmyocardium and even more so as compared to the epicardium. A transmural gradient expression of human I_{Ks} or I_{Kr} has yet to be reported, but it has been shown to be non-significant in canine tissues (without β-AR stimulation)[49]. In our study, β-AR stimulation reduced epicardial APD while I_{Kr} block increased endocardial APD, the combined effect of which would result in increased transmural dispersion of repolarization (Supplemental Fig. 8). This transmural gradient could provide the substrate for functional block and arrhythmias. It is important to note that I_{Ks} did not have a significant impact on the transmural gradient, with or without β-AR stimulation. Thus, it is more likely that the combination of an increased CV from β-AR stimulation and a prolonged APD from I_{Ks} block provide enough repolarization de-synchrony to trigger and sustain TdP in LQT1 patients.

Moreover, while enhanced transmural dispersion is pro-arrhythmic, increased wavelength is anti-arrhythmic, because it requires a much greater amount of tissue to sustain reentry[50,51]. Supplemental Fig. 6 shows that wavelength was increased with every pharmacologic intervention due to both increased CV and APD. Cardiac susceptibility to arrhythmias depends on the balance between wavelength and transmural heterogeneity.

Computational stimulation reflects experimental β-AR stimulation and I_{Ks} blockade. The phosphorylation states before and after β-AR stimulation were adjusted to match experimental APs. Despite using a saturating dosage of the I_{Ks} blocker JNJ-303, computational simulation indicated that not all I_{Ks} channels were blocked. We suspect this was due to remaining problems with the O'Hara-Rudy computer model. For example, the model could only support a 20% I_{Kr} block prior to inducing EADs. This was in contrast to experimental data, where even a saturated I_{Kr} blockade did not produce any EADs. While this model was able to recapitulate experimental data obtained during I_{Ks} blockade relatively closely, it still failed to represent I_{Kr} block similar to the original O'Hara-Rudy model. This major difference is likely due to strong cell-cell coupling that is only present when considering tissue response[52]. Alternatively, other repolarizing currents, such as small conductance potassium currents, could be present, which are not currently incorporated in the O'Hara-Rudy computer model. A tissue model is currently being developed using presented experimental data.

Advantages and limitations of a pharmacologic interrogation approach. In most experimental models, isolated whole-cell voltage clamp is the approach of choice when measuring ionic currents. However, it has been shown that for human tissue, which is highly fibrotic especially in less healthy donor hearts, a powerful cell isolation protocol is required. The isolation procedure can become harmful to membrane multiprotein complexes, including ionic currents. Alterations of an I_{Ks} multiprotein complex due to experimental cell isolation procedure is likely[19]. Additionally, the increase of CV from β-stimulation is crucial in the mechanism by which I_{Ks} can induce TdP. Therefore, the model of a coronary perfused wedge preparation represents a powerful approach. Furthermore, recently developed cardiac organotypic slice preparations can further extend these studies of human repolarization because of their abilities to recapitulate both acute and chronic effects of drugs (e.g. chronic α- and β-AR stimulation) in inducing repolarization remodeling[53].

The pharmacologic agents used in this study were highly specific at the concentrations used, as already demonstrated by multiple other groups. However, I_{Kr} conductance is strongly dependent on other channels. Experimental protocols that involve a blockade of the different channels used here can alter their individual effects and were not necessarily fully specific to each of their targets. Therefore, it is important to consider complex context in data interpretation. Nevertheless, despite the lack of specificity of some pharmacologic agents, the magnitude of significance found in this study outweigh the limitations of the approach.

Finally, it is important to take into consideration the high variability of human subjects in this study, such as gender and age. Information on the exact health status of donor hearts was very limited. While most hearts were rejected for transplantation due to age restriction, there were unavoidable samples that had early onset of heart disease but were asymptotic. All available donor hearts (excluding those from cardiac death) were utilized due to the scarcity nature of tissue. Regardless, all hearts used in this study were categorized as non-failing hearts, with expected healthy contractility and β-AR response. Despite these limitations, these hearts represent normal human physiology as close as currently possible.

References

1. Barhanin, J. *et al*. K(V)LQT1 and lsK (minK) proteins associate to form the I(Ks) cardiac potassium current. *Nature* **384**, 78–80 (1996).
2. Sanguinetti, M. C. & Jurkiewicz, N. K. Two components of cardiac delayed rectifier K+ current. Differential sensitivity to block by class III antiarrhythmic agents. *The Journal of general physiology* **96**, 195–215 (1990).
3. Priori, S. G. *et al*. Risk stratification in the long-QT syndrome. *The New England journal of medicine* **348**, 1866–1874 (2003).
4. Schwartz, P. J. *et al*. Prevalence of the congenital long-QT syndrome. *Circulation* **120**, 1761–1767 (2009).
5. Bohnen, M. S. *et al*. Molecular Pathophysiology of Congenital Long QT Syndrome. *Physiological reviews* **97**, 89–134 (2017).
6. Barhanin, J., Attali, B. & Lazdunski, M. IKs, a slow and intriguing cardiac K+ channel and its associated long QT diseases. *Trends in cardiovascular medicine* **8**, 207–214 (1998).
7. Osteen, J. D., Sampson, K. J. & Kass, R. S. The cardiac IKs channel, complex indeed. *Proceedings of the National Academy of Sciences of the United States of America* **107**, 18751–18752 (2010).
8. Bosch, R. F. *et al*. Effects of the chromanol 293B, a selective blocker of the slow, component of the delayed rectifier K+ current, on repolarization in human and guinea pig ventricular myocytes. *Cardiovascular research* **38**, 441–450 (1998).
9. Lu, Z., Kamiya, K., Opthof, T., Yasui, K. & Kodama, I. Density and kinetics of I(Kr) and I(Ks) in guinea pig and rabbit ventricular myocytes explain different efficacy of I(Ks) blockade at high heart rate in guinea pig and rabbit: implications for arrhythmogenesis in humans. *Circulation* **104**, 951–956 (2001).
10. Bosch, R. F. *et al*. beta3-Adrenergic regulation of an ion channel in the heart-inhibition of the slow delayed rectifier potassium current I(Ks) in guinea pig ventricular myocytes. *Cardiovascular research* **56**, 393–403 (2002).
11. Apkon, M. & Nerbonne, J. M. Characterization of two distinct depolarization-activated K+ currents in isolated adult rat ventricular myocytes. *The Journal of general physiology* **97**, 973–1011 (1991).
12. Varro, A. *et al*. The role of the delayed rectifier component IKs in dog ventricular muscle and Purkinje fibre repolarization. *The Journal of physiology* **523**(Pt 1), 67–81 (2000).
13. Lengyel, C. *et al*. Pharmacological block of the slow component of the outward delayed rectifier current (I(Ks)) fails to lengthen rabbit ventricular muscle QT(c) and action potential duration. *British journal of pharmacology* **132**, 101–110 (2001).
14. Towart, R. *et al*. Blockade of the I(Ks) potassium channel: an overlooked cardiovascular liability in drug safety screening? *Journal of pharmacological and toxicological methods* **60**, 1–10 (2009).
15. Li, G. R., Feng, J., Yue, L., Carrier, M. & Nattel, S. Evidence for two components of delayed rectifier K+ current in human ventricular myocytes. *Circulation research* **78**, 689–696 (1996).
16. Jost, N. *et al*. Restricting excessive cardiac action potential and QT prolongation: a vital role for IKs in human ventricular muscle. *Circulation* **112**, 1392–1399 (2005).
17. Beuckelmann, D. J., Nabauer, M. & Erdmann, E. Alterations of K+ currents in isolated human ventricular myocytes from patients with terminal heart failure. *Circulation research* **73**, 379–385 (1993).
18. Veldkamp, M. W., van Ginneken, A. C., Opthof, T. & Bouman, L. N. Delayed rectifier channels in human ventricular myocytes. *Circulation* **92**, 3497–3504 (1995).
19. Yue, L., Feng, J., Li, G. R. & Nattel, S. Transient outward and delayed rectifier currents in canine atrium: properties and role of isolation methods. *The American journal of physiology* **270**, H2157–2168 (1996).
20. Banyasz, T. *et al*. Beta-adrenergic stimulation reverses the I Kr-I Ks dominant pattern during cardiac action potential. *Pflugers Archiv: European journal of physiology* **466**, 2067–2076 (2014).
21. Sanguinetti, M. C., Jurkiewicz, N. K., Scott, A. & Siegl, P. K. Isoproterenol antagonizes prolongation of refractory period by the class III antiarrhythmic agent E-4031 in guinea pig myocytes. Mechanism of action. *Circulation research* **68**, 77–84 (1991).
22. Bennett, P. B. & Begenisich, T. B. Catecholamines modulate the delayed rectifying potassium current (IK) in guinea pig ventricular myocytes. *Pflugers Archiv: European journal of physiology* **410**, 217–219 (1987).
23. Yazawa, K. & Kameyama, M. Mechanism of receptor-mediated modulation of the delayed outward potassium current in guinea-pig ventricular myocytes. *The Journal of physiology* **421**, 135–150 (1990).
24. Holzem, K. M. *et al*. Reduced response to IKr blockade and altered hERG1a/1b stoichiometry in human heart failure. *Journal of molecular and cellular cardiology* **96**, 82–92 (2016).
25. ten Tusscher, K. H., Noble, D., Noble, P. J. & Panfilov, A. V. A model for human ventricular tissue. *American journal of physiology. Heart and circulatory physiology* **286**, H1573–1589 (2004).
26. Grandi, E., Pasqualini, F. S. & Bers, D. M. A novel computational model of the human ventricular action potential and Ca transient. *Journal of molecular and cellular cardiology* **48**, 112–121 (2010).
27. O'Hara, T., Virag, L., Varro, A. & Rudy, Y. Simulation of the undiseased human cardiac ventricular action potential: model formulation and experimental validation. *PLoS computational biology* **7**, e1002061 (2011).
28. Mirams, G. R. *et al*. Prediction of Thorough QT study results using action potential simulations based on ion channel screens. *Journal of pharmacological and toxicological methods* **70**, 246–254 (2014).
29. Glukhov, A. V. *et al*. Transmural dispersion of repolarization in failing and nonfailing human ventricle. *Circulation research* **106**, 981–991 (2010).
30. Lou, Q. *et al*. Transmural heterogeneity and remodeling of ventricular excitation-contraction coupling in human heart failure. *Circulation* **123**, 1881–1890 (2011).
31. Lang, D. *et al*. Arrhythmogenic remodeling of beta2 versus beta1 adrenergic signaling in the human failing heart. *Circulation. Arrhythmia and electrophysiology* **8**, 409–419 (2015).
32. Ng, F. S. *et al*. Adverse remodeling of the electrophysiological response to ischemia-reperfusion in human heart failure is associated with remodeling of metabolic gene expression. *Circulation. Arrhythmia and electrophysiology* **7**, 875–882 (2014).
33. Laughner, J. I., Ng, F. S., Sulkin, M. S., Arthur, R. M. & Efimov, I. R. Processing and analysis of cardiac optical mapping data obtained with potentiometric dyes. *American journal of physiology. Heart and circulatory physiology* **303**, H753–765 (2012).
34. Doshi, A. N. *et al*. Feasibility of a semi-automated method for cardiac conduction velocity analysis of high-resolution activation maps. *Computers in biology and medicine* **65**, 177–183 (2015).
35. Heijman, J., Volders, P. G., Westra, R. L. & Rudy, Y. Local control of beta-adrenergic stimulation: Effects on ventricular myocyte electrophysiology and Ca(2+)-transient. *Journal of molecular and cellular cardiology* **50**, 863–871 (2011).
36. Severi, S., Corsi, C., Rocchetti, M. & Zaza, A. Mechanisms of beta-adrenergic modulation of I(Ks) in the guinea-pig ventricle: insights from experimental and model-based analysis. *Biophysical journal* **96**, 3862–3872 (2009).
37. Oyamada, M. *et al*. The expression, phosphorylation, and localization of connexin 43 and gap-junctional intercellular communication during the establishment of a synchronized contraction of cultured neonatal rat cardiac myocytes. *Experimental cell research* **212**, 351–358 (1994).
38. Veeraraghavan, R. *et al*. Sodium channels in the Cx43 gap junction perinexus may constitute a cardiac ephapse: an experimental and modeling study. *Pflugers Archiv: European journal of physiology* **467**, 2093–2105 (2015).
39. Braam, S. R. *et al*. Repolarization reserve determines drug responses in human pluripotent stem cell derived cardiomyocytes. *Stem cell research* **10**, 48–56 (2013).
40. Antzelevitch, C. Ionic, molecular, and cellular bases of QT-interval prolongation and torsade de pointes. *Europace: European pacing, arrhythmias, and cardiac electrophysiology: journal of the working groups on cardiac pacing, arrhythmias, and cardiac cellular electrophysiology of the European Society of Cardiology* **9**(Suppl 4), iv4–15 (2007).

41. Gallacher, D. J. *et al*. *In vivo* mechanisms precipitating torsades de pointes in a canine model of drug-induced long-QT1 syndrome. *Cardiovascular research* **76**, 247–256 (2007).
42. Harmati, G. *et al*. Effects of beta-adrenoceptor stimulation on delayed rectifier K(+) currents in canine ventricular cardiomyocytes. *British journal of pharmacology* **162**, 890–896 (2011).
43. Rosenbaum, D. M., Rasmussen, S. G. & Kobilka, B. K. The structure and function of G-protein-coupled receptors. *Nature* **459**, 356–363 (2009).
44. Zareba, W. *et al*. Influence of genotype on the clinical course of the long-QT syndrome. International Long-QT Syndrome Registry Research Group. *The New England journal of medicine* **339**, 960–965 (1998).
45. Banyasz, T., Horvath, B., Jian, Z., Izu, L. T. & Chen-Izu, Y. Sequential dissection of multiple ionic currents in single cardiac myocytes under action potential-clamp. *Journal of molecular and cellular cardiology* **50**, 578–581 (2011).
46. Krogh-Madsen, T., Sobie, E. A. & Christini, D. J. Improving cardiomyocyte model fidelity and utility via dynamic electrophysiology protocols and optimization algorithms. *The Journal of physiology* **594**, 2525–2536 (2016).
47. Devenyi, R. A. *et al*. Differential roles of two delayed rectifier potassium currents in regulation of ventricular action potential duration and arrhythmia susceptibility. *The Journal of physiology* (2016).
48. Beau, S. L., Tolley, T. K. & Saffitz, J. E. Heterogeneous transmural distribution of beta-adrenergic receptor subtypes in failing human hearts. *Circulation* **88**, 2501–2509 (1993).
49. Bauer, A. *et al*. Effects of the I(Kr)-blocking agent dofetilide and of the I(Ks)-blocking agent chromanol 293b on regional disparity of left ventricular repolarization in the intact canine heart. *Journal of cardiovascular pharmacology* **39**, 460–467 (2002).
50. Garrey, W. E. The nature of fibrillary contraction of the heart: its relation to tissue mass and form. *Amercian Journal of Physiology* **33**, 397–414 (1914).
51. Panfilov, A. V. Is heart size a factor in ventricular fibrillation? Or how close are rabbit and human hearts? *Heart Rhythm* **3**, 862–864 (2006).
52. Xie, Y., Sato, D., Garfinkel, A., Qu, Z. & Weiss, J. N. So little source, so much sink: requirements for afterdepolarizations to propagate in tissue. *Biophysical journal* **99**, 1408–1415 (2010).
53. Kang, C. *et al*. Human Organotypic Cultured Cardiac Slices: New Platform For High Throughput Preclinical Human Trials. *Scientific reports* **6**, 28798 (2016).

Acknowledgements

The authors wish to gratefully acknowledge Washington Regional Transplant Community, Washington DC and Mid-America Transplant Services, St. Louis, M.O. We are grateful to Dr. Michael Pasque from Washington University School of Medicine, and the families of donors for donating cardiac tissues, which enabled this research program. We gratefully acknowledge funding from the National Institutes of Health grants R01 HL114395 and R01 HL126802 and Leducq Foundation Network of Excellence grant Repolarization HeterogeneitY imaging for personalized Therapy of Heart arrhythmia (RHYTHM).

Author Contributions

C.K., C.G., and I.R.E. conception of research. C.K., C.G., I.R.E. design of research and experiments. C.K., C.G., Y.Q., and J.A.B. performed the wet-lab experiments and analyzed the data. A.B. performed computational simulation based on collected data. C.K. and I.R.E. drafted the manuscript. C.K., A.B., N.T., J.A.B., and I.R.E. edited and revised the manuscript. All co-authors approved the final version of the manuscript.

Additional Information

Supplementary information accompanies this paper at https://doi.org/10.1038/s41598-017-16218-3.

Competing Interests: The authors declare that they have no competing interests.

Publisher's note: Springer Nature remains neutral with regard to jurisdictional claims in published maps and institutional affiliations.